Pseudo-anapole regime in terahertz metasurfaces

Maria V. Cojocari,[1] Anar K. Ospanova,[1,2] Vladimir I. Chichkov,[1]
Miguel Navarro-Cía,[3,4] Andrei Gorodetsky,[3,5,6,*] and Alexey A. Basharin[1,7,8]

[1]*National University of Science and Technology (MISiS),Moscow 119049, Russia*
[2]*Al-Farabi Kazakh National University, Almaty 050040, Kazakhstan*
[3]*School of Physics and Astronomy, University of Birmingham, Birmingham B15 2TT, UK*
[4]*Department of Electronic, Electrical and Systems Engineering, University of Birmingham, Birmingham B15 2TT, UK*
[5]*Department of Chemistry, Imperial College London, London W12 0BZ, UK*
[6]*ITMO University, St. Petersburg 197101, Russia*
[7]*Institute for Theoretical and Applied Electromagnetics RAS, Moscow 125412, Russia*
[8]*Moscow Institute of Physics and Technology, Dolgoprudny, Moscow Region, 117303, Russia*

(Dated: July 15, 2021)

We present the numerical, theoretical, and experimental study of a terahertz metasurface supporting a pseudo-anapole. Pseudo-anapole effect arises when electric and toroidal dipole moments both tend to a minimum, instead of destructive interference between electric and toroidal dipole moments in conventional anapole mode. Such overlap allows resonance suppression of electric type radiation. Thus, it becomes possible to study the multipoles of other families and higher order excitations. We estimate multipoles contribution to the metasurface response via the multipole expansion method. The series is extended with such terms as mean-square radii and multipoles interference. We also study the metasurface geometrical tunability. Via scaling, we demonstrate that it is possible to control the metasurface toroidal and electric responses independently. This in turn proves the fact that these multipoles have different physical origin. Moreover, we demonstrate that proposed metasurface allows excitation of coherent magnetic dipole and electric quadrupole modes which is crucial for planar cavities and lasing spasers in nanophotonics.

I. INTRODUCTION

Metamaterials and metasurfaces are generally periodically arranged resonant elements whose properties allow manipulation of electromagnetic waves at subwavelength scale. Thus, exotic phenomena can be demonstrated in metamaterials such as superresolution, excitation of highly confined surface waves, negative refraction, and cloaking [1, 2]. Usually, the electromagnetic response of metamaterials and metasurfaces is determined by the interaction of electric and magnetic multipoles in metamolecules. However, there are several problems in nanophotonics that require the excitation of high-order multipoles, such as quadrupoles, octopoles, and even multipoles of mean-square radii. High-order multipole resonances feature multilobe radiation patterns with sharp lobes and high Q-factor. Besides, their optical response is caused by strong near fields.

Diffraction theory suggests that scatterers must have dimensions greater than the incoming wavelength and have a complex design for the excitation of higher order multipoles. Hence, practical implementations of such excitation so far consist of several bulk particles coupled to each other by near fields. In these configurations, higher multipoles are masked by stronger dipole moments of electric and magnetic families. Alternatively, higher multipole resonant enhancement is feasible by suppressing the main multipoles while strengthening the desired ones. Thus, Feng *et al*. [3] proposed the concept of an "ideal magnetic dipole scattering", whereby a magnetic dipole moment is isolated in a core/shell dielectric nanoparticle due to the suppression of the electric type of scattering, namely to the anapole mode destructive interference of the resonantly enhanced electric and toroidal dipole moments [4]. Moreover, Terekhov *et al*. demonstrated the excitation of a magnetic octopole in a split dielectric nanocuboid [5]. All-dielectric nanoparticles with voids were used by Zenin *et al*. to attain nearly pure scattering of higher order multipoles at several wavelengths in infrared region. Namely, spheres with different sizes of the voids were used to show prevailing electric or magnetic octopoles scattering. It was also shown experimentally that disks allow the observation of electric octopole and magnetic hexadecapole scattering, depending on the inner diameter [6].

Here, we introduce an alternative method of enhancing higher order multipoles in a terahertz (THz) metasurface. Our approach is to suppress the electric type radiation by nullifying the electric and toroidal multipoles in the same frequency range. Given its unique planar implementation, our solution holds promise for further implementation as efficient higher multipoles interaction enhancer in microwave, THz and nanophotonic metamaterials and metasurfaces. For instance, a planar toroidal metamaterial with low radiating losses resonances is readably achievable [7, 8]. Such metamaterials possess high Q-factor determined by excitation of toroidal dipole moment, that is a separate element of the multipole decomposition [9, 10].

Toroidal and electric dipoles radiate with identical radiation patterns, while they have different current configurations in their origin [11, 12]. Nevertheless, the Cartesian multipole expansion of poloidal currents flowing along torus meridians demonstrates that radiating intensity of electric dipole moment is zero, though intensity of toroidal moment prevails in the system [13]. Moreover, the identity of the radiation patterns of toroidal and electric dipoles leads to a nonradiating

* andrei@itmo.ru

state, called anapole, which is a result of destructive interference between these dipole moments obeying $\boldsymbol{P} = -ik\boldsymbol{T}$, condition (where $\boldsymbol{P}$ is the electric dipole moment, $\boldsymbol{T}$ is the toroidal dipole, and k is the wavenumber) [14, 15].

Since pioneering works on anapole excitation by Fedotov *et al*. [14] and Miroshnichenko *et al*. [15], research efforts have been geared towards novel contributions of anapole nanophotonics [3, 16–18] and their applications: near fields enhancing, extremely high Q-factor [19], transverse scattering [20], switching [21], multipolar cloaking [22], hybrid anapole excitation [23], anapole lasing [24], thermally tunable anapole metasurfaces [25], and higher harmonics generation [20, 26].

II. PSEUDO-ANAPOLE STATE

The anapole state is rather elusive because it is often destroyed by extra-radiated multipoles generated in real metaparticles [8]. Nevertheless, one can stress that the toroidal dipole moment is the compensating factor of the electric dipole radiation in the anapole. Thus, due to the toroidal moment excitation, one has a chance to suppress the radiation of electric one. Similarly, because of so-called moment of mean-square magnetic radius, it is possible to suppress radiation of the magnetic moment [23, 27–30].

Deep insight into the theory of invisibility provides strong correlation between anapole mode and V-th Devaney-Wolf theorem. According to this theorem, if $\boldsymbol{F}$ is any vector field that is continuous and has continuous partial derivatives up to the third order and that vanishes at all points outside its finite volume, the condition $\boldsymbol{J}_{NR} = \dfrac{1}{4\pi i}\dfrac{c}{k}\left(\nabla\times\nabla\times\boldsymbol{F} - k^2\boldsymbol{F}\right) = 0$ ensures that $\boldsymbol{F}$ is nonradiating field and source has nonradiating current $\boldsymbol{J}_{NR}$ [31]. The equivalent current $\boldsymbol{J}_{eq}$ that is generated by the anapole metamolecule must obey the following expression and tends to zero [32]:

$$\boldsymbol{J}_{eq} = \nabla\times\nabla\times\boldsymbol{T} - ik\boldsymbol{P} = 0. \qquad (1)$$

Indeed, this equation is true, when $\boldsymbol{P} = -ik\boldsymbol{T}$, which is the condition of anapole state. In this case electric dipole moment (or toroidal one, which is the same) in anapole condition satisfies the Eq. 1:

$$\boldsymbol{J}_{eq} = \nabla\times\nabla\times\boldsymbol{T} - ik\boldsymbol{T} \equiv \nabla\times\nabla\times\boldsymbol{F} - ik\boldsymbol{F}. \qquad (2)$$

Thus, for a function of $\boldsymbol{T}$, the physics behind is the same as nonradiating function $\boldsymbol{F}$ in Devaney-Wolf theorem.

Here, we propose another solution which always satisfies the Eq. (1), the case of $\boldsymbol{P} = 0$ and $\boldsymbol{T} = 0$. Unlike the reverse condition – maximal $\boldsymbol{P}$ and $\boldsymbol{T}$ – which leads to maximum value of the equivalent current (super dipole) [33], minimal values of $\boldsymbol{P}$ and $\boldsymbol{T}$ also define a non-radiating system with equivalent current tending to zero. We introduce this non-radiating system as ***pseudo-anapole***. In contrary to the conventional anapole, this way we can compensate electric dipole excitation even in non-toroidal planar structures as toroidal moment is expected to be minimum in pseudo-anapole regime. Thus, we can expect electric type radiation to be suppressed to the level of other multipoles leading to excitation of higher order multipoles in the system. We demonstrate this effect in a THz metasurface. Its toroidal and electric responses are significantly suppressed at the resonance frequency so that their far-field intensity tends to zero. Proposed THz metasurface consists of periodically arranged metamolecules, in the shape of the two ϵ-shaped voids [19] in the Nb plate (Fig. 1 (a)).

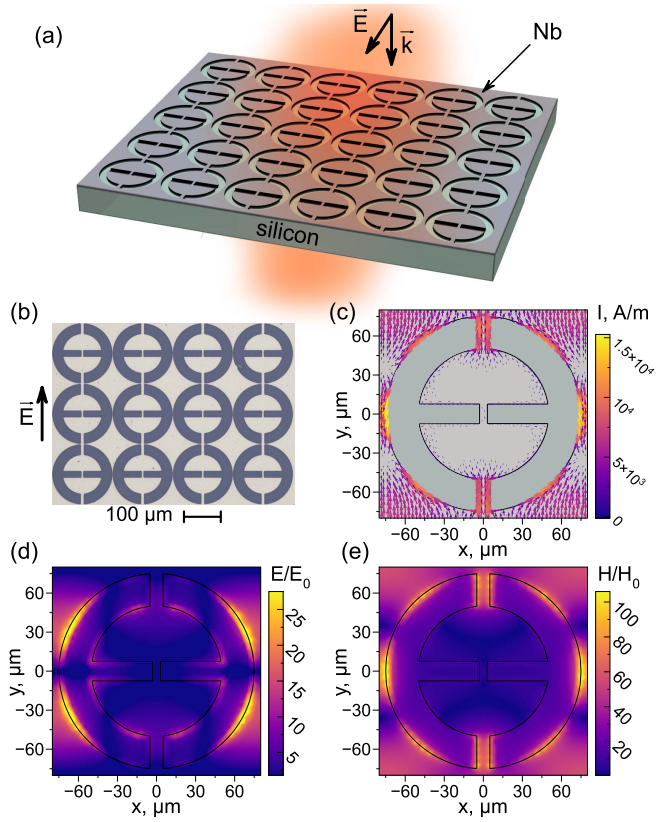

FIG. 1. (a) Illustration of the metasurface, and (b) SEM image of the metasurface fragment, where $\vec{k}$ and $\vec{E}$ denote the propagating direction and polarisation of the incident THz field, respectively. (c) Current distribution in the unit cell of the metasurface at the frequency of 0.8 THz, (d) and (e) are the distributions of electric and magnetic fields at the frequency of 0.8 THz, respectively.

The dimensions of the metamolecules are the following: inner radius is 50 μm, outer radius is 75 μm, central wire width is 6 μm, outer wires are 10 μm wide, the width of the central void strip is 15 μm. We choose these parameters in order to obtain resonance in the THz spectrum below 1 THz.

We simulate the metasurface response with the commercial solver CST Microwave Studio ® using periodical boundary condition. The metasurface is normally excited with $\boldsymbol{E}$-vector polarized along wires of the metamolecules. On the one hand, such configuration is capable of supporting two loops of currents along the voids (Fig. 1 (c)), resulting in toroidal excitation. On the other hand, due to the vertical wires, the electric dipole is excited in the system.

III. EXPERIMENTAL

A. Sample preparation

The experimental metasurface sample was fabricated by deposition of two 100 nm thick niobium films onto the substrate of monocrystalline silicon (001) (Fig. 1 (b)) [34, 35]. Sputter deposition on direct current of a niobium target (99.99% clean) was used for deposition. Vacuum chamber was pumped to a constant pressure below 7.5×10^{-8} mbar. During the process of sputtering, argon (99.9995% clean) operating pressure was 5×10^{-3} mbar; discharge current was 500 mA; the velocity of niobium sputtering was 0.6 nm/s.

Metasurface geometry profile was obtained by optical photolithography. Mask was developed from photoresist S1813G2. Its exposure was obtained in laser lithographer Heidelberg uPG 501. Niobium was etched in high frequency plasma in Sentech SI 591 Compact plasma etcher. Discharge power was 50 W, plasma was ignited in reactive gases mixture of SF_6 and O_2 in the ratio of 5:1 and resulting pressure of 9×10^{-2} mbar; a built-in laser interferometer controlled the stopping moment of the etching.

B. Experimental setup and measurement

Experimental setup was a home built THz time-domain spectrometer (TDS) pumped with amplified Ti:Sapphire laser system (Coherent Astrella), providing pulses of 40 fs duration at 800 nm wavelength with the repetition rate of 4 kHz. Laser Quantum Tera-SED semiconductor biased large area emitter was used as a THz source, and 1mm thick ZnTe crystal as an electro-optic medium in a balanced detection scheme. The setup was dry-air purged provided broadband operation covering the spectrum between 0.1 and 3.5 THz with signal to noise ratio $\geqslant 3 \times 10^2$ and amplitude dynamic range of $\geqslant 10^5$. To get the experimental values of the metasurface transmission, the signal measured through the metasurface on the substrate was normalised to the transmission of the bare high-resistive silicon substrate $S_{21} = \dfrac{T_{sam}}{T_{sub}}$.

Similarly, in the simulation, transmission of the metasurface was normalised to one of a bare substrate, to match the experimental conditions. To obtain the exact values of the substrate complex dielectric permittivity in the THz range $\varepsilon_1(f) + i\varepsilon_2(f)$, for precise simulation, as this value strongly depends on the dopants concentration, its properties were retrieved as [36]:

$$\varepsilon_1(f) + i\varepsilon_2(f) = (n(f) + ik(f))^2, \tag{3}$$

where

$$\mathrm{Re}(n(f)) = 1 + \frac{c\Delta\phi(f)}{2\pi f d}, \tag{4}$$

and

$$\mathrm{Im}(n(f)) = -\frac{c}{2\pi f d} \cdot \ln\left(\frac{T_{sub}(f)}{T_{ref}(f)} \frac{(n(f)-1)^2}{4 \cdot n(f)}\right), \tag{5}$$

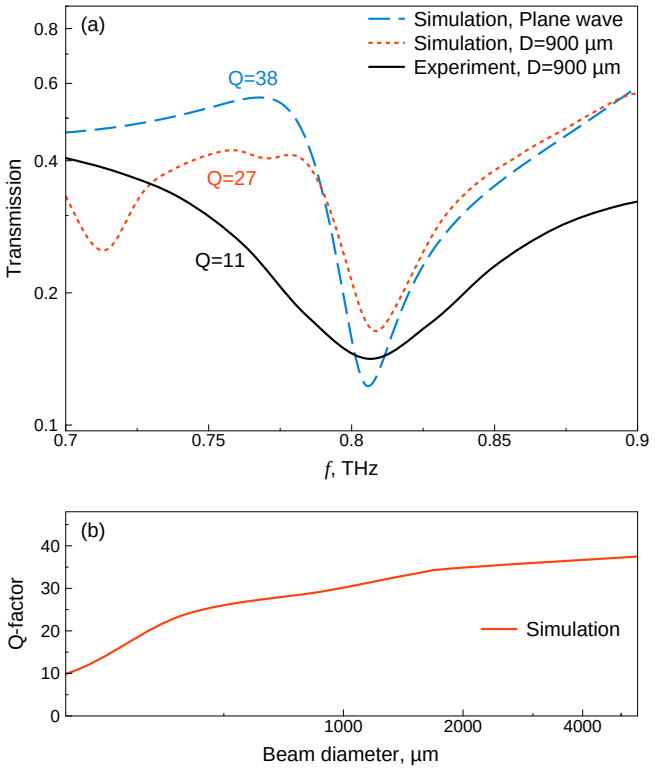

FIG. 2. (a) Simulated plane wave (blue short dashed), simulated limited area (red dashed) and measured limited area (green solid) transmission of the material in the THz range. (b) Simulated 0.8 THz resonance Q-factor as a function of beam diameter.

T_{sub} and T_{ref} are the complex spectra of the substrate and reference signals, and d is the thickness of the substrate. Retrieved substrate properties are shown in the appendix.

IV. RESULTS AND DISCUSSION

In the transmission spectrum, we observe a resonance dip at the frequency of 0.8 THz, matching the experimentally observed one (Fig. 2 (a)). The Q-factor of metasurface response in experimental and theoretical case differ due to several reasons; the main reason is linked to the spectral collapse of the metamolecules coherence [37]. So-called spectral line collapse arises due to reflection of the magnetoinductive waves running across the sample (which manifests itself isolated at 0.72 THz in the D = 900 μm case of Fig. 2 (a)), from the unexcited metamolecules [1]. The use of such collective effect has been widely discussed in the context of lasing spasers that is planar coherent source of electromagnetic energy [37, 38]. Here, we numerically demonstrate such phenomenon by decreasing the number of illuminated metamolecules varying the incident beam size (Fig. 2 (b)). For this case we use open boundary condition and simulate a truncated array instead of infinite array in the case labelled as plane wave excitation. Q-factor of the transmission resonance depends on the incident beam diameter, and changes from ~ 10 for the

beam with 400 μm diameter to ~ 40 for the infinitely large beam (Fig. 2 (b)). Pseudo-anapole at 0.8 THz arises in the array and we have taken into account the interactions between metamolecules in the multipoles interference. Similarly to the lattice anapole effect [39], we can conclude that our effect is also a lattice pseudo-anapole effect. Further spectral broadening might occur due to the fabrication imperfections [40] and non-normal incidence of the tightly focused THz beam in the experiment [41], as outlined in [42] for other quasi-optical metasurfaces.

To further study the reason for the resonance occurrence, we simulate the field and current distributions in the metamolecule at the resonance frequency. The electric field is concentrated more on the periphery of the metamolecule (Fig. 1 (d)), while the magnetic field is found around the side wires and reaches very high values – over $H/H_0 \approx 106$ times the incident field at 0.8 THz (Fig. 1 (e)). The excited currents along the voids (Fig. 1 (c)) are similar to the shape of the poloidal currents on the torus meridians. In addition, the currents on lateral and central parts of voids flow in the opposite direction. Such current configuration suppresses toroidal dipole moment and due to closed current loops, we can expect diminishing electric moment intensity.

For detailed investigation of the resonance nature, we perform multipole expansion of currents excited in each metamolecule for the following multipoles (Fig. 3): $\boldsymbol{P}$ - electric dipole, $\boldsymbol{M}$ - magnetic dipole, $\boldsymbol{T}$ - toroidal dipole moments; $\boldsymbol{Q^e}$ – electric, $\boldsymbol{Q^m}$ – magnetic, and $\boldsymbol{Q^T}$ – toroidal quadrupoles, respectively and multipoles of the next order, called mean-square radii of $\boldsymbol{R^{m\text{-}}}$ – magnetic, $\boldsymbol{R^T}$ – toroidal and $\boldsymbol{RQ^{m\text{-}}}$ – magnetic quadrupole, respectively [27, 29].

We use Cartesian multipole expansion. All multipole modes are expressed by integrals over particle volume with different moments of current $\boldsymbol{j}$. Thus, dipole moments are given as:

$$\begin{aligned} P_\alpha &= \frac{i}{\omega}\int\limits_V j_\alpha d^3 r \\ M_\alpha &= \frac{1}{2}\int\limits_V (\boldsymbol{r}\times\boldsymbol{j})_\alpha d^3 r \\ T_\alpha &= \frac{1}{10}\int\limits_V \left[(\boldsymbol{j}\cdot\boldsymbol{r})\, r_\alpha - 2r^2 j_\alpha\right] d^3 r, \end{aligned} \tag{6}$$

Quadrupole moments are calculated as:

$$\begin{aligned} Q^e_{\alpha\beta} &= \frac{i}{\omega}\int\limits_V \left[r_\alpha j_\beta + r_\beta j_\alpha - \tfrac{2}{3}\delta_{\alpha\beta}(\boldsymbol{r}\cdot\boldsymbol{j})\right] d^3 r \\ Q^m_{\alpha\beta} &= \frac{1}{3}\int\limits_V \left[(\boldsymbol{r}\times\boldsymbol{j})_\alpha r_\beta + (\boldsymbol{r}\times\boldsymbol{j})_\beta r_\alpha\right] d^3 r \\ Q^T_{\alpha\beta} &= \frac{1}{42}\int\limits_V \left[4(\boldsymbol{r}\cdot\boldsymbol{j})\, r_\alpha r_\beta + 2\delta_{\alpha\beta}(\boldsymbol{j}\cdot\boldsymbol{r})r^2 - 5r^2\left(r_\alpha j_\beta + r_\beta j_\alpha\right)\right] d^3 r \end{aligned} \tag{7}$$

and mean square radii can be obtained with:

$$\begin{aligned} R^m_\alpha &= \frac{i\omega}{20}\int\limits_V r^2 (\boldsymbol{r}\times\boldsymbol{j})_\alpha d^3 r \\ R^T_\alpha &= \frac{1}{280}\int\limits_V \left[3r^4 j_\alpha - 2r^2(\boldsymbol{r}\cdot\boldsymbol{j})\, r_\alpha\right] d^3 r \\ RQ^m_{\alpha\beta} &= \frac{i\omega}{42}\int\limits_V r^2\left[(\boldsymbol{r}\times\boldsymbol{j})_\alpha r_\beta + (\boldsymbol{r}\times\boldsymbol{j})_\beta r_\alpha\right] d^3 r, \end{aligned} \tag{8}$$

where $\alpha, \beta = x, y, z$.

Although radiation intensity of the waves generated by mean square radii multipoles is low, for the correct characterisation of the system, their contributions must be considered. The total field radiated by an infinite metasurface is obtained by summing of contributions from all metamolecules. Due to almost plane wave excitation at normal incidence, all metamolecules oscillate in phase. The total field radiated by the array can be obtained as [39, 43]:

$$\boldsymbol{E}_S = \frac{1}{\Delta^2}\int\limits_{Array} d^2 r\, \boldsymbol{E}(\boldsymbol{r}), \tag{9}$$

where Δ is the unit cell area.

The far-field radiated by multipoles can be written as:

$$\begin{aligned} \boldsymbol{E}_S = \frac{\mu_0 c^2}{2\Delta^2}\Big[& ik\left(\boldsymbol{P}_\parallel + ik\boldsymbol{T}_\parallel + ik^3\boldsymbol{R}^T\right) \\ & + ik\hat{\boldsymbol{R}}\times\left(\boldsymbol{M}_\parallel + ik\boldsymbol{R}^m_\parallel\right) + k^2\left(\left(\boldsymbol{Q}^e + ik\boldsymbol{Q}^T\right)\cdot\hat{\boldsymbol{R}}\right)_\parallel \\ & - \frac{k^2}{2}\hat{\boldsymbol{R}}\times\left(\left(\boldsymbol{Q}^m + ik\boldsymbol{R}\boldsymbol{Q}^m\right)\cdot\hat{\boldsymbol{R}}\right)_\parallel\Big] e^{-ik\hat{\boldsymbol{R}}} \end{aligned} \tag{10}$$

where the subscript $(...)_\parallel$ denotes the projection of the corresponding vector onto the plane of the array and $\hat{\boldsymbol{R}}$ is the distance from the array to the observer.

The reflected and transmitted fields of metasurface are given by:

$$\begin{aligned} \boldsymbol{E}_r &= \left[\boldsymbol{E}_S\right]_{\boldsymbol{n}=-\boldsymbol{k}} \\ \boldsymbol{E}_t &= \left[\boldsymbol{E}_S\right]_{\boldsymbol{n}=\boldsymbol{k}} + \boldsymbol{E}_{inc}, \end{aligned} \tag{11}$$

where $\boldsymbol{E}_{inc}$ is the incoming field.

The result of performed multipole expansion is presented in the Fig. 3 near the resonance frequency of 0.8 THz. We note that electric and toroidal moments have the shape of a Fano resonance, accompanied by minima and maxima. We choose metamolecule geometry so that dips of toroidal and electrical dipole moments coincide and tend to minimum at 0.8 THz (Fig. 3 (b)). This leads to the pseudo-anapole regime introduced previously. Thus, the pseudo-anapole mode can play the role of a reducing factor for radiation of the electric type. We note that interference intensity of electric and toroidal dipole moments, as well as mean square radius of the toroidal moment, tends to a minimum (Fig. 4 (b)). However, we stress that interference of magnetic dipole and mean

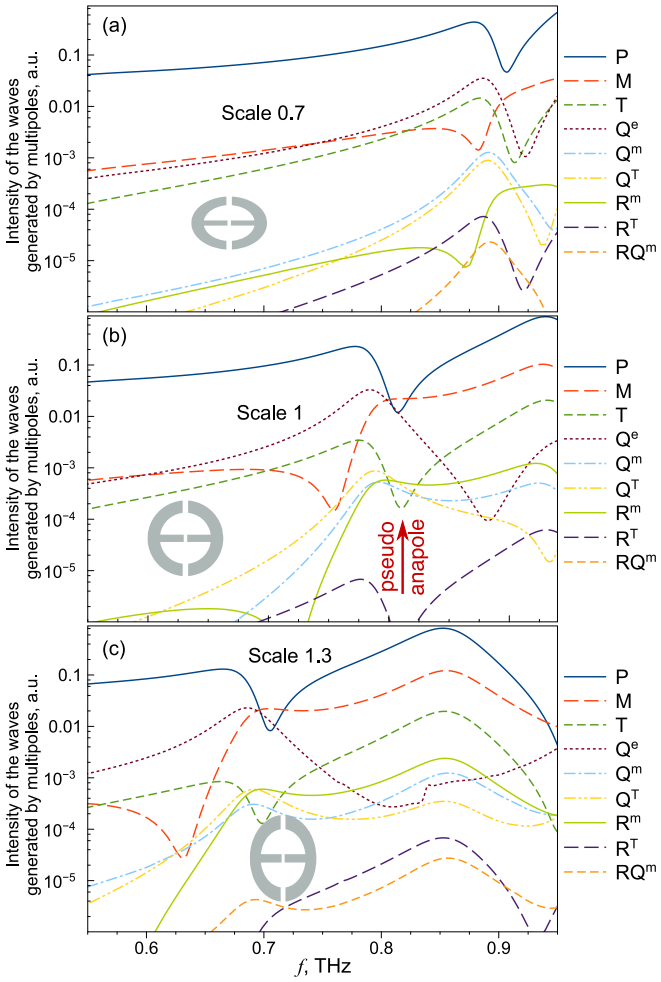

FIG. 3. Intensity of the waves generated by multipoles for the geometries vertically scaled by the factor of (a) 0.7, (b) 1 and (c) 1.3, respectively. Dipole modes are shown in dashed magentas, quadrupoles – in dotted beige, and higher order multipoles in green dash-dotted curves, respectively.

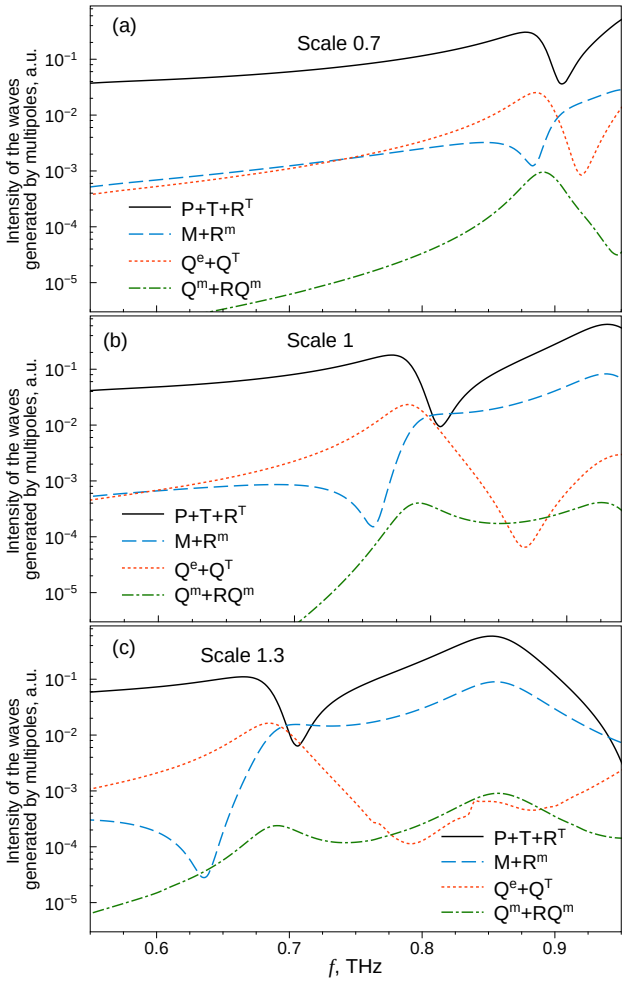

FIG. 4. Interference between multipoles for the geometries of (a) scale 0.7, (b) scale 1 and (c) scale 1.3, respectively.

square radius of magnetic dipole, as well as interference of electric and toroidal quadrupoles determines the response of the metasurface and tends to the maximum (Fig. 4 (a)).

Moreover, the results of multipole expansion demonstrate domination of magnetic dipole which oscillates coherently in all metamolecules. The reason of spectral collapse is attributed to magnetoinductive surface waves. In the case of plane wave or very broad incident beam magnetoinductive waves radiate only in the plane. But in the case of smaller beam diameters, magnetoinductive waves are scattered at non-excited lateral metamolecules resulting in scattering losses and, accordingly, leading to Q-factor suppression (Fig. 2 (b)) [37].

Hereafter, we discuss the evolution of excited multipoles in the system with respect to the metamolecules geometry. To study this dependence, we change the metamolecule proportionally in the vertical direction and increase its vertical size by the factors of 0.7 and 1.3. For smaller scaling factor of 0.7, the metamolecule is compressed and poloidal currents flow in a smaller volume, causing toroidal moment arise at higher frequencies. It is blueshifted from electric dipole moment.(Fig. 3 (a)). For the larger value of the scaling factor, 1.3, the minimum of the toroidal moment is redshifted with respect to the minimum of the electric moment (Fig. 3 (c)). This is manifested in the fact that interference between the mentioned dipole moments occurs with lower intensity in the case of oblate metamolecules (Fig. 4 (a)) and with higher intensity in case of prolate ones (Fig. 4 (c)). Thus, via vertical scaling, one can control toroidal and electric responses of the metasurface independently. This ability proves the fact that electric and toroidal multipoles have different nature and can be tuned independently. This outcome addresses a widely discussed and unsettled narrative [17].

Pseudo-anapole is a promising effect for suppressing the electric type radiation. This is primarily relevant for the problems, where it is necessary to extract dipoles of another family, for example, magnetic dipoles, from the spectra, like in magnetic Purcell effect [44]. It can also be applied to the structures with the strong magnetic field localisation as soon as THz inductance formation is based on toroidal re-

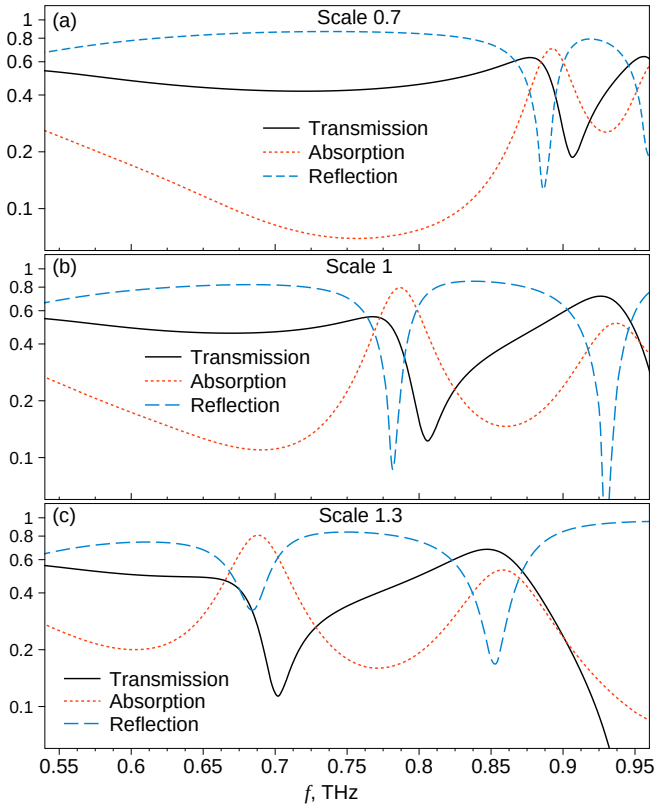

FIG. 5. Transmission,absorption and reflection spectra for the geometries of vertical (a) scale 0.7, (b) scale 1 and (c) scale 1.3.

sponse [3, 21, 45, 46]. Moreover, a magnetic dipole couples to an electric quadrupole in a manner similar to induced spectral narrow Kerker lattice effect [47, 48], and this coupling is promising for effects that are enabled by the metasurfaces. All previous demonsrations of the effect were performed in 3D all-dielectric and plasmonic structures. In contrast, our solution is quasi-planar.

V. CONCLUSIONS

In conclusion, we have proposed and examined theoretically, numerically and experimentally a THz metasurface with sharp resonance dip in the transmission spectrum. The pronounced dip is mainly defined by higher-order multipoles due to the introduced pseudo-anapole regime. Unlike other cases where the dipole moment is suppressed nonresonantly, as for example in magnetic dipole particles, the pseudo-anapole is a resonant effect. We have shown both numerically and analytically that the resonance at the frequency of ~ 0.8 THz corresponds to pseudo-anapole regime with resonantly suppressed electric and toroidal dipole moments and illuminated magnetic dipole and electric quadrupole. We have introduced a way to tailor these moments independently, by geometrical scaling. Thus, we introduce a regime in which one can explore multipoles of higher order, e.g., the response of the proposed metasurface is defined by magnetic dipole and electric quadrupole moments. For the proposed metasurface, we demonstrated spectral collapse effect, increasing with reduction of the incident beam diameter. We prove that by means of such coherent metasurface we obtained enhanced Q-factor important for such modern applications in metamaterial research and nanophotonics as lasing spasers.

ACKNOWLEDGEMENTS

A.G. acknowledges support from Russian Foundation for Basic Research [Grant No 18-07-01492-a], A.K.O. acknowledges support from RSF [Grant No 20-72-00016] for mutipoles decomposition analysis works, M. N.-C. acknowledges support from the Royal Society [Grant No. IEC\NSFC\191104], V.I.C acknowledges the Ministry of Science and Higher Education of the Russian Federation (Project No. 0718-2020-0025) for support in sample fabrication. A.A.B acknowledges the RSF (Project No. 21-19-00138) for support in simulations, EPSRC [Grant No. EP/S018395/1] and the European Union Horizon 2020 research and innovation programme [Grant No. 777714]. MISiS team acknowledge support from the Ministry of Education K2-2018-015. A.G. thanks Magicplot LLC for providing a copy of MagicPlot Pro plotting and fitting software used for preparation of all figures in the manuscript.

Appendix: Silicon substrate properties

Complex refractive index and complex permittivity of samples are shown in Fig. 6.

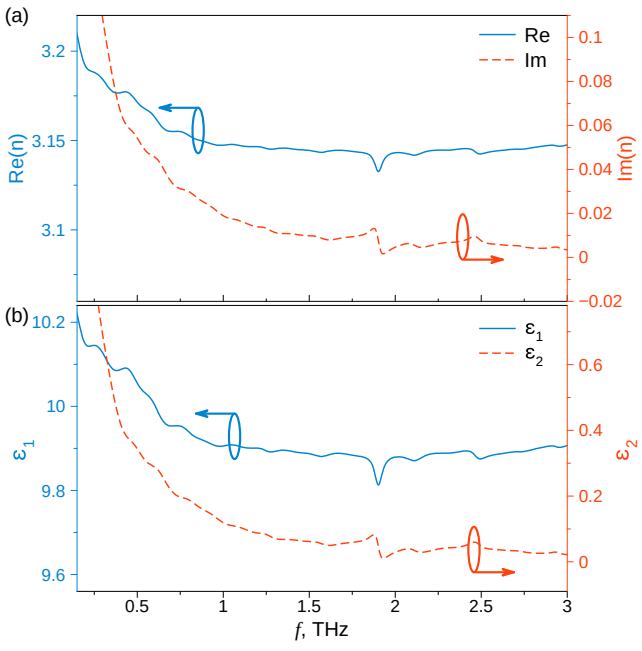

FIG. 6. Retrieved silicon substrate properties in the THz range: (a) complex refractive index, and (b) complex permittivity.

[1] L. Solymar and E. Shamonina, *Waves in metamaterials* (Oxford University Press, 2009).

[2] C. Simovski and S. Tretyakov, *An Introduction to Metamaterials and Nanophotonics* (Cambridge University Press, 2020).

[3] T. Feng, Y. Xu, W. Zhang, and A. E. Miroshnichenko, Ideal Magnetic Dipole Scattering, Phys. Rev. Lett. **118**, 173901 (2017).

[4] B. Cappello, A. K. Ospanova, L. Matekovits, and A. A. Basharin, Mantle cloaking due to ideal magnetic dipole scattering, Sci. Rep. **10**, 2413 (2020).

[5] P. D. Terekhov, A. B. Evlyukhin, D. Redka, V. S. Volkov, A. S. Shalin, and A. Karabchevsky, Magnetic Octupole Response of Dielectric Quadrumers, Laser Photon. Rev. **14**, 1900331 (2020).

[6] V. A. Zenin, C. E. Garcia-Ortiz, A. B. Evlyukhin, Y. Yang, R. Malureanu, S. M. Novikov, V. Coello, B. N. Chichkov, S. I. Bozhevolnyi, A. V. Lavrinenko, and N. A. Mortensen, Engineering nanoparticles with pure high-order multipole scattering, ACS Photonics **7**, 1067 (2020), https://doi.org/10.1021/acsphotonics.0c00078.

[7] T. Kaelberer, V. A. Fedotov, N. Papasimakis, D. P. Tsai, and N. I. Zheludev, Toroidal Dipolar Response in a Metamaterial, Science **330**, 1510 (2010).

[8] N. Papasimakis, V. A. Fedotov, V. Savinov, T. A. Raybould, and N. I. Zheludev, Electromagnetic toroidal excitations in matter and free space, Nat. Mater. **15**, 263 (2016).

[9] E. E. Radescu and G. Vaman, Exact calculation of the angular momentum loss, recoil force, and radiation intensity for an arbitrary source in terms of electric, magnetic, and toroid multipoles, Phys. Rev. E **65**, 046609 (2002).

[10] V. Dubovik and V. Tugushev, Toroid moments in electrodynamics and solid-state physics, Phys. Rep. **187**, 145 (1990).

[11] G. N. Afanasiev and Y. P. Stepanovsky, The electromagnetic field of elementary time-dependent toroidal sources, J. Phys. A. Math. Gen. **28**, 4565 (1995).

[12] N. Pavlov, I. Stenishchev, A. Ospanova, P. Belov, P. Kapitanova, and A. Basharin, Toroidal Dipole Mode Observation In Situ, Phys. status solidi **257**, 1900406 (2020).

[13] K. Marinov, A. D. Boardman, V. A. Fedotov, and N. Zheludev, Toroidal metamaterial, New J. Phys. **9**, 324 (2007).

[14] V. A. Fedotov, A. V. Rogacheva, V. Savinov, D. P. Tsai, and N. I. Zheludev, Resonant transparency and non-trivial non-radiating excitations in toroidal metamaterials, Sci. Rep. **3**, 1 (2013).

[15] A. E. Miroshnichenko, A. B. Evlyukhin, Y. F. Yu, R. M. Bakker, A. Chipouline, A. I. Kuznetsov, B. Luk'yanchuk, B. N. Chichkov, and Y. S. Kivshar, Nonradiating anapole modes in dielectric nanoparticles, Nat. Commun. **6**, 8069 (2015).

[16] K. V. Baryshnikova, D. A. Smirnova, B. S. Luk'yanchuk, and Y. S. Kivshar, Optical Anapoles: Concepts and Applications, Adv. Opt. Mater. **7**, 1801350 (2019).

[17] V. Savinov, N. Papasimakis, D. P. Tsai, and N. I. Zheludev, Optical anapoles, Commun. Phys. **2**, 69 (2019).

[18] M. Gupta and R. Singh, Toroidal metasurfaces in a 2D flatland, Rev. Phys. **5**, 100040 (2020).

[19] A. A. Basharin, V. Chuguevsky, N. Volsky, M. Kafesaki, and E. N. Economou, Extremely high Q-factor metamaterials due to anapole excitation, Phys. Rev. B **95**, 035104 (2017).

[20] H. K. Shamkhi, K. V. Baryshnikova, A. Sayanskiy, P. Kapitanova, P. D. Terekhov, P. Belov, A. Karabchevsky, A. B. Evlyukhin, Y. Kivshar, and A. S. Shalin, Transverse Scattering and Generalized Kerker Effects in All-Dielectric Mie-Resonant Metaoptics, Phys. Rev. Lett. **122**, 193905 (2019).

[21] M. Gupta, Y. K. Srivastava, and R. Singh, A Toroidal Metamaterial Switch, Adv. Mater. **30**, 1704845 (2018).

[22] A. K. Ospanova, G. Labate, L. Matekovits, and A. A. Basharin, Multipolar passive cloaking by nonradiating anapole excitation, Sci. Rep. **8**, 12514 (2018).

[23] B. Luk'yanchuk, R. Paniagua-Domínguez, A. I. Kuznetsov, A. E. Miroshnichenko, and Y. S. Kivshar, Hybrid anapole modes of high-index dielectric nanoparticles, Phys. Rev. A **95**, 063820 (2017).

[24] J. S. Totero Gongora, A. E. Miroshnichenko, Y. S. Kivshar, and A. Fratalocchi, Anapole nanolasers for mode-locking and ultrafast pulse generation, Nat. Commun. **8**, 15535 (2017).

[25] E. Takou, A. C. Tasolamprou, O. Tsilipakos, Z. Viskadourakis, M. Kafesaki, G. Kenanakis, and E. N. Economou, Anapole Tolerance to Dissipation Losses in Thermally Tunable Water-Based Metasurfaces, Phys. Rev. Appl. **15**, 014043 (2021).

[26] G. Grinblat, Y. Li, M. P. Nielsen, R. F. Oulton, and S. A. Maier, Enhanced Third Harmonic Generation in Single Germanium Nanodisks Excited at the Anapole Mode, Nano Lett. **16**, 4635 (2016).

[27] N. A. Nemkov, A. A. Basharin, and V. A. Fedotov, Electromagnetic sources beyond common multipoles, Phys. Rev. A **98**, 023858 (2018).

[28] E. Takou, A. C. Tasolamprou, O. Tsilipakos, and E. N. Economou, Dynamic anapole in metasurfaces made of sculptured cylinders, Phys. Rev. B **100**, 085431 (2019).

[29] E. A. Gurvitz, K. S. Ladutenko, P. A. Dergachev, A. B. Evlyukhin, A. E. Miroshnichenko, and A. S. Shalin, The High-Order Toroidal Moments and Anapole States in All-Dielectric Photonics, Laser Photon. Rev. **13**, 1800266 (2019).

[30] A. K. Ospanova, A. Basharin, A. E. Miroshnichenko, and B. Luk'yanchuk, Generalized hybrid anapole modes in all-dielectric ellipsoid particles [Invited], Opt. Mater. Express **11**, 23 (2021).

[31] A. J. Devaney and E. Wolf, Radiating and Nonradiating Classical Current Distributions and the Fields They Generate, Phys. Rev. D **8**, 1044 (1973).

[32] G. Labate, A. K. Ospanova, N. A. Nemkov, A. A. Basharin, and L. Matekovits, Nonradiating anapole condition derived from Devaney-Wolf theorem and excited in a broken-symmetry dielectric particle, Opt. Express **28**, 10294 (2020).

[33] P. D. Terekhov, K. V. Baryshnikova, A. S. Shalin, A. Karabchevsky, and A. B. Evlyukhin, Resonant forward scattering of light by high-refractive-index dielectric nanoparticles with toroidal dipole contribution, Opt. Lett. **42**, 835 (2017).

[34] A. V. Pronin, M. Dressel, A. Pimenov, A. Loidl, I. V. Roshchin, and L. H. Greene, Direct observation of the superconducting energy gap developing in the conductivity spectra of niobium, Phys. Rev. B **57**, 14416 (1998).

[35] Geoffrey Chanda, *TERAHERTZ AND INFRARED SPECTROSCOPY OF NOVEL SUPERCONDUCTORS*, Ph.D. thesis (2014).

[36] N. V. Petrov, M. S. Kulya, A. N. Tsypkin, V. G. Bespalov, and A. Gorodetsky, Application of Terahertz Pulse Time-Domain Holography for Phase Imaging, IEEE Trans. Terahertz Sci. Technol. **6**, 464 (2016).

[37] V. A. Fedotov, N. Papasimakis, E. Plum, A. Bitzer, M. Walther, P. Kuo, D. P. Tsai, and N. I. Zheludev, Spectral Collapse in Ensembles of Metamolecules, Phys. Rev. Lett. **104**, 223901 (2010).

[38] N. I. Zheludev, S. L. Prosvirnin, N. Papasimakis, and V. A. Fedotov, Lasing spaser, Nat. Photonics **2**, 351 (2008).

[39] P. D. Terekhov, V. E. Babicheva, K. V. Baryshnikova, A. S. Shalin, A. Karabchevsky, and A. B. Evlyukhin, Multipole analysis of dielectric metasurfaces composed of nonspherical nanoparticles and lattice invisibility effect, Phys. Rev. B **99**, 045424 (2019).

[40] S. Lepeshov, A. Gorodetsky, A. Krasnok, N. Toropov, T. A. Vartanyan, P. Belov, A. Alú, and E. U. Rafailov, Boosting Terahertz Photoconductive Antenna Performance with Optimised Plasmonic Nanostructures, Sci. Rep. **8**, 6624 (2018).

[41] S. Freer, A. Gorodetsky, and M. Navarro-Cia, Beam Profiling of a Commercial Lens-Assisted Terahertz Time Domain Spectrometer, IEEE Trans. Terahertz Sci. Technol. **11**, 90 (2021).

[42] M. Navarro-Cía, V. Pacheco-Peña, S. A. Kuznetsov, and M. Beruete, Extraordinary THz Transmission with a Small Beam Spot: The Leaky Wave Mechanism, Adv. Opt. Mater. **6**, 1701312 (2018).

[43] V. Savinov, V. A. Fedotov, and N. I. Zheludev, Toroidal dipolar excitation and macroscopic electromagnetic properties of metamaterials, Phys. Rev. B **89**, 205112 (2014).

[44] P. Albella, M. A. Poyli, M. K. Schmidt, S. A. Maier, F. Moreno, J. J. Sáenz, and J. Aizpurua, Low-Loss Electric and Magnetic Field-Enhanced Spectroscopy with Subwavelength Silicon Dimers, J. Phys. Chem. C **117**, 13573 (2013).

[45] M. Gupta and R. Singh, Toroidal versus Fano Resonances in High Q planar THz Metamaterials, Adv. Opt. Mater. **4**, 2119 (2016).

[46] M. Gupta, V. Savinov, N. Xu, L. Cong, G. Dayal, S. Wang, W. Zhang, N. I. Zheludev, and R. Singh, Sharp Toroidal Resonances in Planar Terahertz Metasurfaces, Adv. Mater. **28**, 8206 (2016).

[47] V. E. Babicheva and A. B. Evlyukhin, Metasurfaces with Electric Quadrupole and Magnetic Dipole Resonant Coupling, ACS Photonics **5**, 2022 (2018).

[48] V. E. Babicheva and A. B. Evlyukhin, Analytical model of resonant electromagnetic dipole-quadrupole coupling in nanoparticle arrays, Phys. Rev. B **99**, 195444 (2019).